DOI 10.1007/s11141-014-9533-6
Radiophysics and Quantum Electronics, Vol. 57, No. 7, December, 2014
(Russian Original Vol. 57, No. 7, July, 2014)

DEVELOPMENT OF WAVEGUIDE SEMICONDUCTOR SWITCHES OF MICROWAVE RADIATION IN THE 70- AND 260-GHz RANGES

M. L. Kulygin,[1] * V. I. Belousov,[1] G. G. Denisov,[1,2] A. A. Vikharev,[1] V. V. Korchagin,[1] A. V. Kuzin,[1] E. A. Novikov,[1] and M. A. Khozin[1]

UDC 537.52

We have developed, manufactured, and studied experimentally prototypes of microwave switches operated in the 70- and 260-GHz frequency ranges and controlled by pulses of optical laser radiation. The results of their numerical simulation by the finite-difference time-domain (FDTD) method are presented, along with the design parameters of the prototypes. The switch speed is equal to 1 ns, and the microwave tuning frequency range amounts to about 10%. The process of switching with the use of a low-cost semiconductor optical laser (with a wavelength of 532 nm and a continuous-wave power of 200 MW) is demonstrated experimentally at a switched-radiation frequency of 266.68 *GHz.*

1. INTRODUCTION

In this work, we consider a semiconductor waveguide switch of microwave radiation, which is designed to modulate and switch the flux of energy of coherent microwave radiation with preserving the mutual coherence of wave packets at the output. The simplified principle of operation of such a switch, which has been known since 1950 [1], is illustrated in Fig. 1. The active element of the switch is a plate of a semiconductor, e.g., silicon (Si). In the initial state, at room temperature and in the absence of external fields, the semiconductor demonstrates electrodynamic properties which are similar to a dielectric with a low ohmic loss. The input flux of the radiation generated by a source of the microwave electromagnetic field passes through the semiconductor plate to the switch output with almost no changes. Matching for the required frequency is achieved by fitting the plate width d. The switching process is controlled using pulses of optical radiation which creates stimulated photoconductivity in a thin layer at the semiconductor boundary. As a result, this semiconductor acquires electric conductivity which is close to that of metals. In this case, the input flux of the microwave energy reflects almost completely, i.e., switching occurs. The appearance of stimulated photoconductivity and its relaxation in the absence of the external optical radiation is a rather fast process with a typical duration of about several microseconds (for silicon) and even nanoseconds (for GaAs) [2].

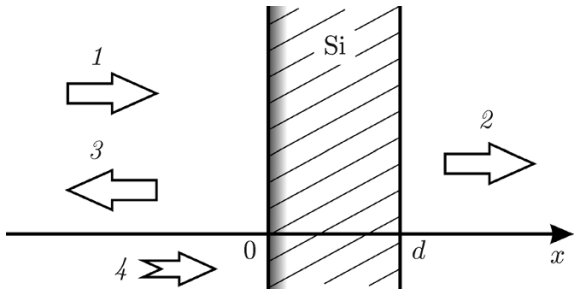

Fig. 1. Simplified operation principle of the semiconductor microwave switch: microwave input source (*1*), output microwave radiation (*2*), reflected microwave radiation (*3*), and laser radiation (*4*).

* kmaxim@appl.sci-nnov.ru

[1]Institute of Applied Physics of the Russian Academy of Sciences; [2]N. I. Lobachevsky State University of Nizhny Novgorod, Nizhny Novgorod, Russia. Translated from Izvestiya Vysshikh Uchebnykh Zavedenii, Radiofizika, Vol. 57, No. 7, pp. 568–579, July 2014. Original article submitted February 4, 2014; accepted July 31, 2014.

The controlled semiconductor element can be a part of a resonance waveguide structure or a quasioptical structure, which allows one theoretically to operate at frequencies of tens and hundreds of gigahertz, as well as at kilo- and megawatt levels of the transmitted microwave power with no risk of thermal destruction and an acceptable loss level. The waveguide band-stop filter described comprehensively in [3] can be chosen as such a structure. The main advantage of such a filter is the presence of a single deep resonance in a wide frequency range. This resonance allows one to suppress significantly the output radiation in a certain narrow frequency band (the "off" state). Laser illumination of the semiconductor plate, which is a resonator element, allows one to detune reversibly the resonance for some time (the "on" state). However, addition of a semiconductor plate to the filter structure changes significantly all quantitative parameters, namely, the frequency, the Q-factor, the number of resonances, and the frequency tuning range. Analytical estimates of the geometry and numerical calculations of the amplitude-frequency characteristic of a band-stop filter in [3] are not suitable for a switch, i.e., controlled band-stop filter. The main reason for this is the fact that any semiconductor plate, even an infinitesimally thin one, has two medium–air interfaces, which reflect the electromagnetic field significantly. Moreover, the thickness of even a relatively thin GaAs plate (about 100 μm thick, since it is not feasible to consider a thinner plate for reasons of physical strength) with the dielectric permittivity $\varepsilon = 12.9$ at a frequency of 70 GHz turns out to be of the order of the field wavelength in the dielectric. This modifies the resonant frequency even greater compared with the filter without a plate. The switch frequency is tuned by means of a mechanical screw by about 10%, which exceeds the width of the filter tuning range by ten times [3].

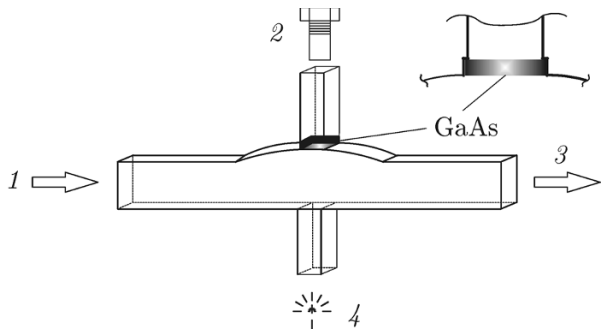

Fig. 2. Design of the microwave switch: input microwave radiation (*1*), a tuning screw (*2*), output microwave radiation (*3*), and a laser (*4*).

The design of the switch is shown in Fig. 2. A standard rectangular waveguide is used at the input and output of the switch. Its dimensions amount to 3.6×1.8 mm and 0.864×0.432 mm for frequency ranges of 70 GHz and 260 GHz, respectively (the IEA WR3 standard). A semiconductor GaAs plate is mounted near the upper aperture (see Fig. 2) of the resonator channel. The laser radiation arrives at the bottom face of the plate through the opposite (bottom) cutoff channel (see Fig. 2) and passes through the resonator. The optimal plate thickness is approximately 200 μm [4]. In the experiments, the plate thickness was 174 μm [4, 5] and 210 μm at frequencies of 70 GHz and 260 GHz, respectively. The screw for mechanical frequency adjustment was located above the semiconductor plate.

2. CALCULATION BY THE FINITE-DIFFERENCE TIME-DOMAIN (FDTD) METHOD

In the process of calculating and optimizing the switch geometry, we use a modification of the well-known finite-difference time-domain (FDTD) method of numerical integration of the Maxwell equations [6–8]. Waveguide switches employ the lower modes of rectangular waveguides with zero index along one of the transverse coordinates. Therefore, the problem is two-dimensional in terms of coordinates. In the system of Maxwell equations (1a) and (1b), we allow for the electric current (1c) expressed via the total mobility μ of the generalized charge carriers in the semiconductor plate and their density N:

$$\operatorname{rot} \mathbf{E} = -\frac{1}{c}\frac{\partial \mathbf{H}}{\partial t}, \tag{1a}$$

$$\operatorname{rot} \mathbf{H} = \frac{\varepsilon}{c}\frac{\partial \mathbf{E}}{\partial t} + \frac{4\pi}{c}\mathbf{j}, \tag{1b}$$

$$\mathbf{j} = eN(t, \mathbf{r})\mu \mathbf{E}. \tag{1c}$$

To simplify the numerical model, charge carriers in the semiconductor are rendered anonymous. To

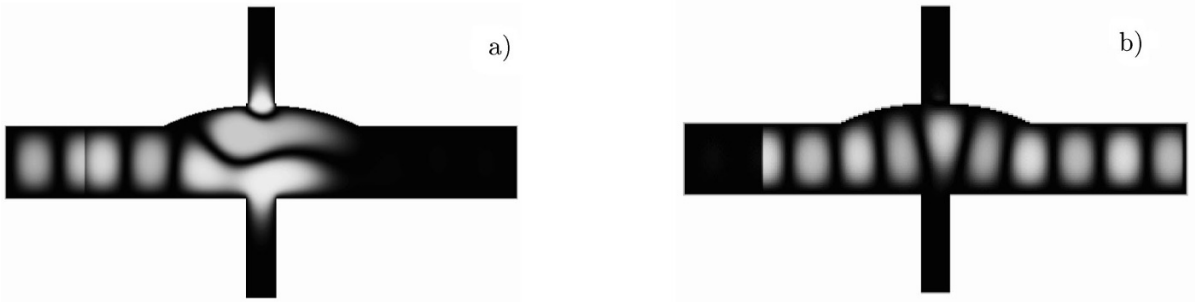

Fig. 3. Field distribution in the switch at resonance in the "closed" state (*a*) and off resonance in the "open" state (*b*).

calculate their number density, we use time-dependent equation which describes the effects of diffusion, relaxation, and excitation of photoconductivity by external laser radiation:

$$\frac{\partial N}{\partial t} = D\,\Delta N + g(\mathbf{r},t) - G_1\,(N - N_{\rm p}). \tag{2}$$

Here, D is the ambipolar-diffusion coefficient in the semiconductor [2], the coefficient G_1 of the first-order relaxation, which plays the main role, is calculated in the preliminary experiment on the semiconductor luminescence relaxation, and $N_{\rm p}$ is the equilibrium number density of carriers in the used semiconductor at room temperature [2]. The particle flow is absent at the semiconductor boundary, which corresponds to the condition $\nabla N = 0$. The internal photoelectric effect, i.e., an increase in the charge-carrier number density with time as matter absorbs light (allowing for the laser radiation attenuation in the bulk of the semiconductor), is described by the equation

$$g(r_\perp, t) = i\exp(-\alpha r_\perp)\theta(t - t_0, \tau). \tag{3}$$

The photoeffect constant is given by the formula $I = \alpha W_p \eta/(S\tau W_q)$, where the inverse skin depth α corresponds to the characteristic width of the photoconductivity layer in the semiconductor for a given wavelength of the laser radiation (optical or IR lasers are used usually), W_p is the laser-pulse energy, W_q is the quantum energy, τ is the pulse duration, θ is a step function, and $r_\perp$ is the distance to the semiconductor surface. A typical beam area S is equal to about 1 mm^2, and η is the photoeffect efficiency, which in practice is equal to approximately 50%.

Solutions of nonstationary nonlinear problems for a one-dimensional switch are given in [9, 10]. A typical solution of a nonlinear nonstationary problem, which corresponds to the two-dimensional switch, is shown in Fig. 3*a*. It is a pattern of the instantaneous distribution of the electric field in the switch in the "closed" stage, i.e., when the field at the output is equal to zero, and the signal is not transmitted through the switch. A standing wave is observed in the resonator, which is achieved by fitting the switch geometry to the specified frequency. By sending a pulse of the control laser radiation (or, vice versa, turning the laser off and waiting for photoconductivity relaxation), we obtain the opposite, i.e., "open", state of the switch (see Fig. 3*b*). In this state, the input signal passes through the switch to the output almost without any changes, and the resonance is destroyed. The depth of the resonance, i.e., attenuation of the power at the output relative to the power at the input in the "closed" state is equal to approximately 30 dB for $Q \approx 300$ with allowance for the ohmic loss. In the resonance state, three field antinodes are observed along the vertical axis in the center of the resonator, similar to the case of the band-stop filter [3]. The GaAs plate is located at the crossing of the resonator and the top section of the cutoff waveguide (Fig. 3*a*). The switching speed is equal to about 1 ns, which is determined by the time of photoconductivity relaxation in the semiconductor and the Q-factor of the resonator [11].

The problem of optimization of the switch is reduced to optimization of its amplitude-frequency characteristic. The main criterion for the optimal amplitude-frequency characteristic $A(f)$ is the presence

of a deep solitary resonance in the specified operating frequency band Δf. The FDTD method allows one to obtain the dynamics of the electromagnetic-field components in the domain of real numbers. This allows one to find the amplitude-frequency characteristic of the switch in one calculation procedure. To obtain the minimum numerical error of finding the amplitude-frequency characteristic within a given frequency band during an optimal calculation time, one should feed a time-limited pulse, which predominantly contains the required frequencies, to the input of the switch. The initial conditions for the fields and currents are equal to zero at the time $t = 0$. The pulse usually has the Gaussian envelope and sinusoidal filling at the center frequency f_0 of the operating band:

$$E_{\text{input}}(\mathbf{r}_\perp, t) = E_{\perp \text{TE10}}(\mathbf{r}_\perp) \sin(2\pi f_0 t) \exp[-4\pi^2 \Delta f^2 (t - t_0)^2]. \tag{4}$$

The envelope cutoff at the initial time $t = 0$ is chosen at the level $\exp(-2)$. Based on these considerations, the time t_0 of the onset of the Gaussian envelope maximum is determined. It is desirable to select the center frequency f_0 of the operating band near the center frequency of the FDTD method [6, 8] to ensure the minimum possible calculation error.

The amplitude-frequency characteristic of the switch in the stationary state is determined as the ratio of the Fourier transform of the signal intensity integral at the output to the output signal power as a function of the frequency. Integration is performed over cross sections at the input and output of the switch. Due to the presence of the single-mode waveguide at the input and output, the amplitude-frequency characteristic is described in the simplest way:

$$A(f) = \left| \int_0^{t_{\max}} \int_{S_{\perp\text{output}}} [\mathbf{E}, \mathbf{H}] \, \mathrm{d}\mathbf{S}_\perp \exp(2\pi i f t) \, \mathrm{d}t \right|^2 \Bigg/ \left| \int_0^{t_{\max}} \int_{S_{\perp\text{input}}} [\mathbf{E}, \mathbf{H}] \, \mathrm{d}\mathbf{S}_\perp \exp(2\pi i f t) \, \mathrm{d}t \right|^2. \tag{5}$$

Due to the energy conservation law,

$$A(f) < 1 \tag{6}$$

at any frequency in the switch with the ohmic loss.

This inequality also serves as the necessary condition of the calculation adequacy. The calculation end time is usually chosen experimentally since in the resonance design, the rate of solution damping depends on the properties of the resonator under consideration. The simplest criteria for the right choice of the calculation end time are the absence of a small-scale quasi-sinusoidal modulation of the amplitude-frequency characteristic near the resonances (the so-called calculation artifacts) and compliance with condition (6).

3. 70-GHz RADIATION SWITCH

The external appearance of a 70-GHz radiation switch is shown in Fig. 4. It is assembled of two copper pieces with a cut along a wide waveguide wall. One piece is a smooth cover, while the other serves as a base for all switch channels. Despite the fact that this design is not optimal from the viewpoint of the ohmic loss, its manufacturing is relatively simple and about 2.5 times as cheap as its optimal counterpart with the conventional bisection cut in the middle of the main waveguide channel parallel to the narrow waveguide wall. Further experiments showed that in the frequency range near 70 GHz (and, therefore, at lower frequencies), a simple-to-manufacture design version with a non-optimal cut is quite operable (Fig. 4), whereas such a simplification is unacceptable in the frequency range near 260 GHz (and, therefore, above that), because the fundamental resonance is so small that it becomes hard to discern against the general background of a significant ohmic loss.

A preliminary experiment with the switch is performed without a laser: the presence of the resonance within the required frequency band, the resonance depth and Q-factor, and the frequency tuning range are checked. The most accurate experiment with the 70-GHz radiation switch was performed using an MVNA vector panoramic complex (manufactured in France). Its results are shown in Fig. 5. The depth of the

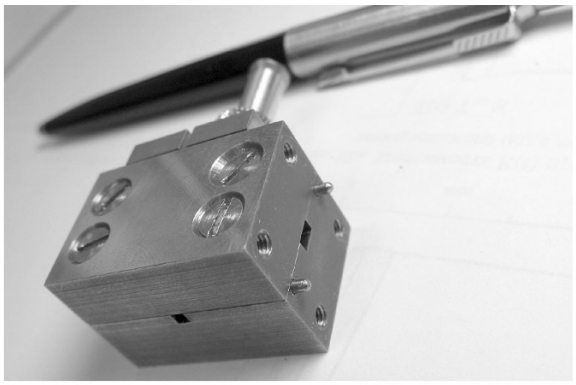

Fig. 4. 70-GHz radiation switch.

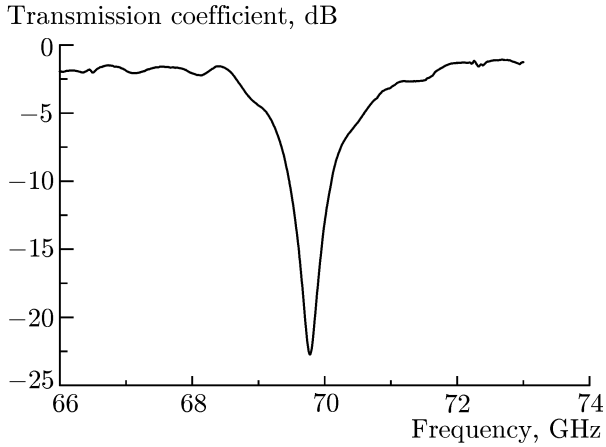

Fig. 5. Resonance curve of the 70-GHz radiation switch.

resonance was about −23 dB in the range 66–72 GHz (with mechanical adjustment using the screw), which is only 7 dB worse than the calculated resonance depth equal to −30 dB for the resonator without a cut. This justifies manufacturing of a resonator with a nonoptimal cut in the chosen frequency range and, consequently, makes the switch design less expensive.

The main experiment [4, 5] was performed using a SpectraPhysics laser cascade (manufactured in USA), i.e., a source of pulses with a duration of 100 fs, a pulse repetition rate of 75.4 MHz, a typical energy of 10 nJ in each pulse, and a wavelength of 780 nm of the envelope filling. The pulses responding to the control laser radiation with the following parameters were obtained at the switch output: a front duration of about 1 ns, a fall duration of 2 ns, a repetition period of 13.6 ns (corresponding to 75.4 MHz), and a filling frequency of 70.3 GHz. When coherent radiation is fed to the switch input, all wave packets at the output are nearly coherent with each other, i.e., the phases of high-frequency filling in all packets are interrelated. Thus, the switch does not introduce any significant phase distortions to the switched radiation. This is especially important for coherent nondestructive spectroscopy, when samples are irradiated with radiation having minimum power, with the possibility of observations in a certain range of frequencies, whereas the direct use of coherent radiation allows one to see the image only at one frequency. With the use of the switch, the range of operating frequencies can be sufficiently wide without a decrease in the sensitivity of the coherent spectrometer.

4. DEVELOPMENT OF THE 260 GHz RADIATION SWITCH

As the initial waveguide for the switch, we choose a standard IEA WR3 waveguide, which has the dimensions 0.864×0.432 mm and is usually used to transmit the single-mode radiation in the frequency band 220–330 GHz. As an option aimed at increasing the power of the switched signal, we also consider a standard WR4 waveguide, which has the dimensions 1.092×0.546 mm and is usually used in the frequency band 170–260 GHz. A typical power range for the needs of spectroscopy is from 0.01 W to 40 W. Calculations of the switches were performed by the FDTD method, but the procedure of geometry optimization was automated, in contrast to manual optimization for the 70-GHz radiation switch. The main difficulty in optimization of the resonance structure of the switch is its low conditionality, i.e., the absence of convergence when iterative synthesis procedures, which are similar to those in [12, 13] are used. On the other hand, the modern computing technology level and relative simplicity of the electrodynamic system of the switch allow one to perform FDTD calculations rather fastly. Indeed, it only suffices to obtain the best amplitude-frequency characteristic (i.e., one with the deep solitary resonance) in the absence of a laser. Therefore, we have decided to optimize the switch geometry by brute-forcing of the main geometric parameters automatically.

For this purpose, the calculation procedure of the FDTD method was simplified as much as possible:

all the nonlinear processes (photoeffect, relaxation of photoconductivity, and diffusion of charge carriers in the semiconductor) were excluded. We allowed for the constant dielectric permittivity of the semiconductor, the loss in the semiconductor, and the finite conductivity of the copper walls and use the unsplit perfectly matched layer (UPML) for the boundary conditions [7, 8]. The two-dimensional Cartesian coordinate grid was used.

The amplitude-frequency characteristic was calculated and analyzed in the frequency range 230–290 GHz. To estimate the profile of the characteristic, one can use the simplest functional $S[A(f)]$, which is the numerical estimate of the specified amplitude-frequency characteristic $A(f)$:

$$S[A(f)] = A_0 \left(1 + \sum_{i=1}^{N} \frac{A_i f_0^n}{|f_i - f_0|^n} \right)^{-1}. \tag{7}$$

Here, we assume that the curve $A(f)$ has N resonances, A_i is the absolute value of the depth of the ith resonance in logarithmic scale (i.e., in dB), f_i is the depth of the ith resonance, and the resonance with zero subscript is the deepest. The positive number n is chosen experimentally in the calculations. The functional vanishes in the presence of an infinite number of resonances in the specified frequency band. A greater value of the functional corresponds to the better amplitude-frequency characteristic, i.e., the better set of geometric parameters.

A finite calculation time of 10 ns was found experimentally. It corresponded to approximately 2500 periods of the electromagnetic field with a center frequency of 260 GHz. During this time, the amplitude-frequency characteristic $A(f)$, which is calculated using Eq. (5), becomes stationary and small oscillations (artifacts of the nonstationary method) disappear. The optimized FDTD calculation with the functional of the estimate of the amplitude-frequency characteristic and the choice of optimal solution yields about 1 solution per minute per each processor core of a modern personal computer (manufactured in 2012–2013). Thus, approximately $3 \cdot 10^5$ solutions can be found and analyzed in one month of continuous calculations using this procedure. A typical instrument error of a milling machine, which is equal to 20 μm and was achieved by us in 2012, was chosen as the parameter-variation increment.

5. SYNTHESIS OF THE RESONATOR USING THE FDTD METHOD

The initial design of the switch to be optimized is shown in Fig. 6*a*. Similar to the band-stop filter [3], this switch is a resonator based on an adiabatic widening of a rectangular waveguide, which is located between two sections of a regular waveguide. The geometry of the symmetric resonator of the switch is determined by two circular arcs (3 independent parameters) and 5 additional quantities: parameters of the cutoff channels and the thickness of the semiconductor plate, i.e., by eight parameters in total. During one month ($3 \cdot 10^5$ calculations), each parameter can take, on the average, five different values, which was realized in the preliminary calculation. It turned out that the center frequency of the resonance curve was determined almost completely by the thickness of the semiconductor plate. The influence of the plate on the frequency is determined by the following rule: a decrease in thickness by 1 μm leads to an increase in frequency by approximately 1 GHz, whereas the other parameters of the resonance vary only slightly. Thus, one can shift the frequencies of most resonance curves by the required 260 GHz almost without any changes.

Preliminary calculations showed that the optimal profile of the adiabatic resonator widening in the switch is zero, i.e., the widening is absent in the optimal switch. This statement has not been proven rigorously: it is a result of exhausting a finite number of parameter values in some reasonable range. Thus, the optimized switch geometry (Fig. 6*b*) is rid of an essential engineering feature of a band-stop filter, namely, a resonator based on the widening of a regular rectangular waveguide. The presence of a semiconductor plate mounted across the cutoff channel at a certain distance from the initial regular waveguide turned out to be sufficient to form the resonator in the switch.

Only five parameters in the switch design were left for optimization. The final optimization procedure looks as follows. Amplitude-frequency characteristic (5) is calculated by the FDTD method on the basis

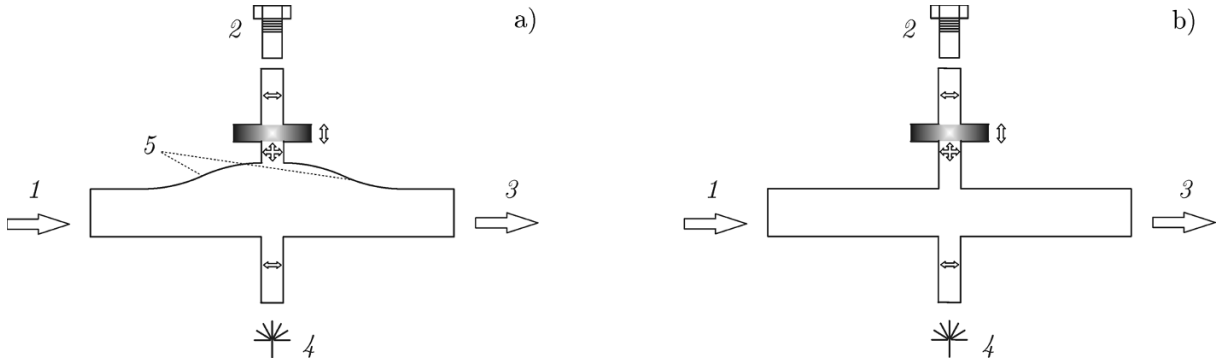

Fig. 6. Design of the 260-GHz radiation switch before optimization (*a*) and with optimization (*b*): input microwave radiation (*1*), adjustment screw (*2*), output microwave radiation (*3*), laser (*4*), and two circular arcs (*5*).

of the initial set of parameters. The deepest resonance in it is chosen, and an attempt is made to shift it to 260 GHz by varying the plate thickness. The obtained amplitude-frequency characteristic is estimated using functional (7). The value of the functional and the corresponding set of parameters are recorded and further sorted. The sets of parameters, which correspond to the "best" amplitude-frequency characteristics, are proposed as optimal sets. Examples of "good" amplitude-frequency characteristics with the functional values close to unity are shown in Fig. 7*a*. Examples of "bad" amplitude-frequency characteristics with the functional values close to 0 are shown in Fig. 7*b*. The set of "good" amplitude-frequency characteristics include the curves with only one deep resonance (whose depth does not exceed −20 dB for the copper WR3 waveguide at 260 GHz). Other resonances are few, they are shallow (no more than several dB), and/or located far from the fundamental resonance. The set of "bad" amplitude-frequency characteristics include the curves with either several deep resonances or a great number of resonances.

The best set of parameters (Fig. 7*a*, left-hand plot) in the presence of the calculated solitary resonance with a depth of −28 dB at a frequency of 259.8 GHz was used for the design based on the initial WR3 waveguide to develop drawings, test manufacturing and assembling techniques, and manufacture operable switch prototypes. An attempt to optimize the design with the WR4 waveguide was also made, but without success. The amplitude-frequency characteristics of the design based on the WR4 waveguide, which were obtained in the numerical experiment, were significantly worse than those in the case with the WR3 waveguide, which is explained by the fact that the WR4 waveguide is not suitable for the use near the upper frequency boundary of the single-mode high-Q wave transmission, which is equal to 260 GHz.

6. EXPERIMENTS WITH THE 260-GHz RADIATION SWITCH

The 260-GHz radiation switch is manufactured by analogy with waveguide components of the IEA WR3 standard (USA) to ensure their compatibility. Figure 8 shows the external appearance of such a switch compared with the standard WR3 waveguide transition. The main visible difference between the switch and the waveguide is the presence of holes for the semiconductor plate and the frequency adjustment screw at the center of the side surface. The switch is made of copper. The experimental amplitude-frequency characteristics of the switch in the states "off/closed" (solid line) and "on/open" (dashed line) are shown in Fig. 9. The amplitude-frequency characteristics in these two states coincide everywhere, excluding the region of the fundamental resonance with a width of several gigahertz and the center at 266.68 GHz. The main mismatch with the calculations (Fig. 7) is a relatively low transmission coefficient off resonance, which is equal to about −2 dB, and the mismatch of the center frequency. In Fig. 9, the experimental value of the resonance depth at a center frequency of 266.68 GHz is equal to about −14 dB, which is quite sufficient for experiments with a nanosecond laser.

To demonstrate the switching effect, we performed a simplified experiment with a low-cost semi-

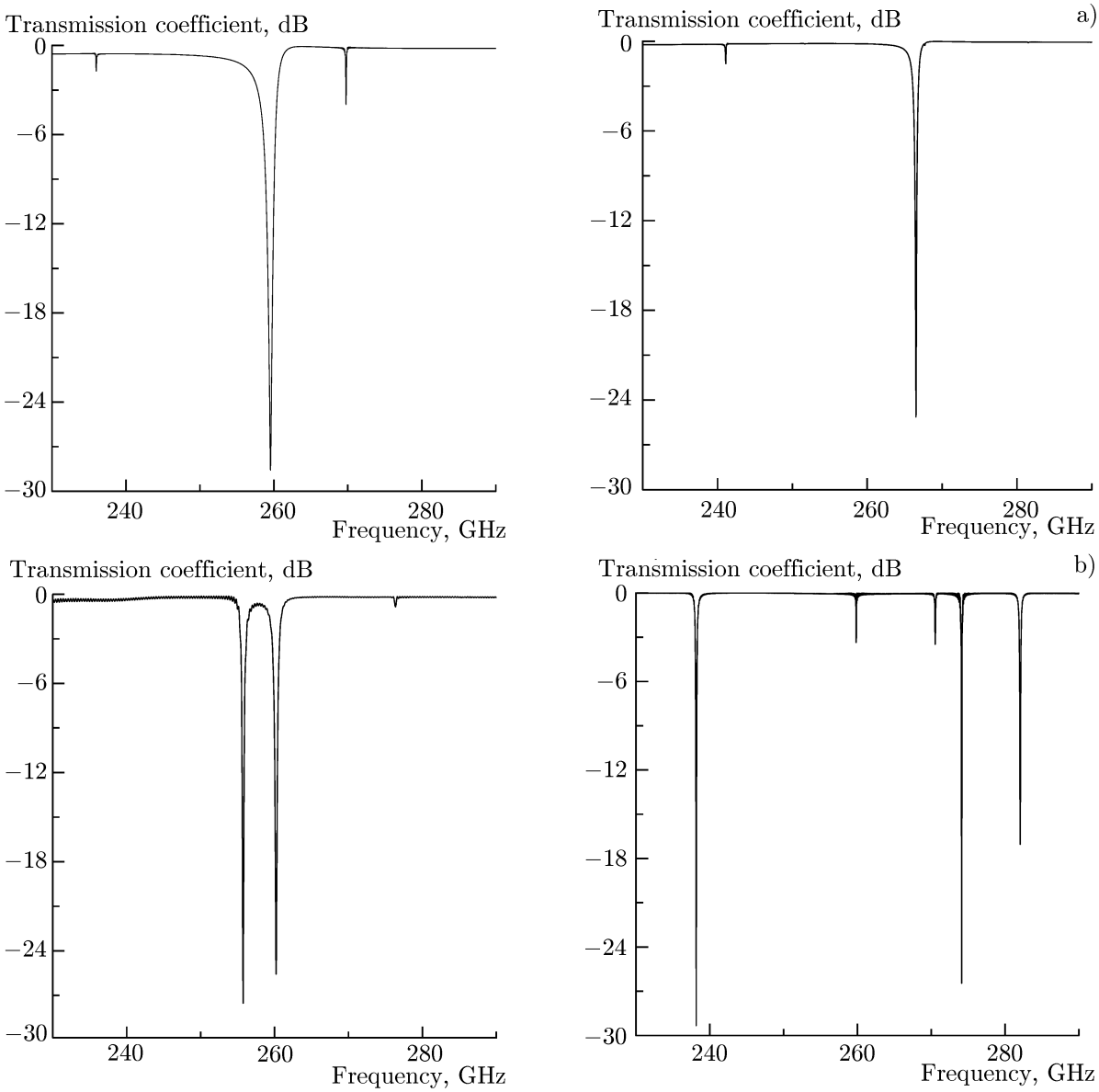

Fig. 7. Examples of "good" (*a*) and "bad" (*b*) amplitude-frequency characteristics in the resonator synthesis process.

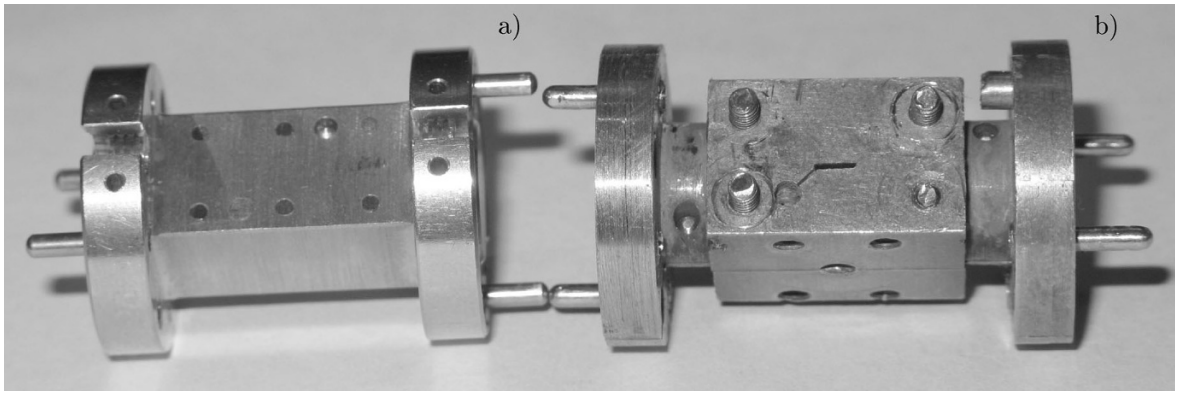

Fig. 8. Standard IEA WR3 waveguide (*a*) and the 260 GHz radiation switch (*b*).

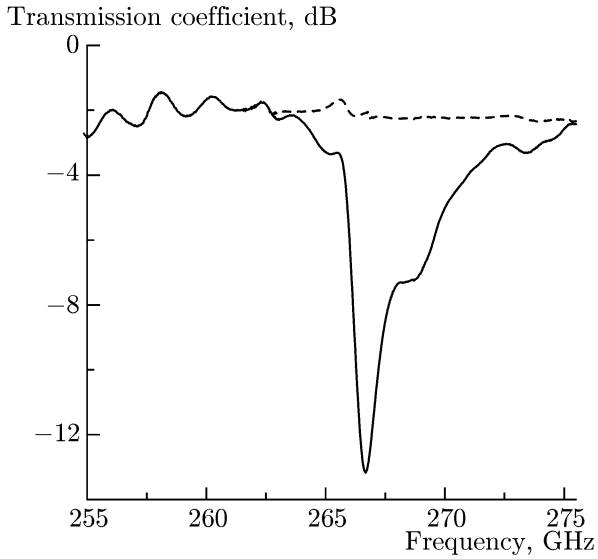

Fig. 9. Experimental amplitude-frequency characteristic of the 260-GHz radiation switch in the initial state (off/close; solid line) and in the case of resonance suppression with the screw (on/open; dashed line).

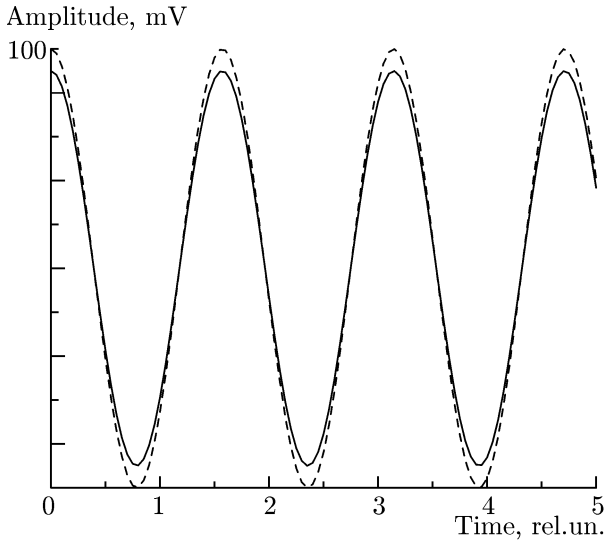

Fig. 10. Variation in the detector signal in the case of laser turning-off: the detector signal in the absence (solid line) and presence (dashed line) of lasing.

conductor laser which produced radiation with a wavelength of 532 nm and a power of about 200 mW in the continuous-wave regime. The overall dimensions of such a laser are relatively small, and it can be focused on the plate manually. We used a microwave source of an MVNA panoramic indicator with a power of about 500 μW in the manual regime without frequency sweeping and with visual recording of the panoramic-detector signal on an oscilloscope. The laser beam was directed through the bottom hole (Fig. 6) of the cutoff channel to the semiconductor plate and was interrupted manually to produce laser pulses. As a response, relatively slow (with a scale of about 100 ms) and relatively weak (about 10%) variations in the amplitude of the amplified and modulated (with a frequency of 1 kHz) detector signal were observed on the oscilloscope display (see Fig. 10). The modulation frequency is determined by the modulator of the MVNA panoramic-indicator. The solid line shows the detector signal at a center resonant frequency of 266.68 GHz in the absence of lasing. The signal amplitude was equal to about 100 mV and was determined by the MVNA amplifier. The dashed line shows the detector signal when the laser radiation falls on the plate. Despite the simplified nature of the experiment and the impossibility to record fast processes, the simplest effect of modulation of 266.68-GHz microwave radiation by the method of laser detuning of the resonator has been demonstrated. We plan to perform an experiment with an industrial nanosecond laser.

7. CONCLUSIONS

In this paper, we have reported on the development, manufacturing, and studies of nanosecond semiconductor switches of microwave radiation in the 70- and 260-GHz frequency ranges, which are controlled by laser pulses. Adequacy of the used numerical model based on the modified FDTD method was confirmed in a series of experiments. The FDTD method allows one to synthesize the resonator at the up-to-date level of computational techniques and avoid typical problems of convergence of the continuous optimization procedure [13] by passing over to the discrete exhaustion of the values of the design parameters. The switch resonator does not need the waveguide widening, which is necessary for the band-stop filter [3].

Wide possibilities of tuning the operating frequency of the microwave switch, the value of which turned out to be no less than 10% [5, 11], were demonstrated. The switch for the 70-GHz frequency range was manufactured and tested successfully with the laser which generated pulses with a duration of 100 fs and

an energy of 10 nJ at a wavelength of 870 μm. The speed of switch operation was equal to about 1 ns [11]. We manufactured a prototype of the switch for the 260-GHz frequency range, in which we demonstrated the simplest effects of modulation of microwaves at a frequency of 266.68 GHz in the case of controlling by a low-cost semiconductor laser with a wavelength of 532 nm and a continuous-wave power of 200 mW.

We plan to perform experiments with stationary industrial nanosecond lasers. Since the presence of the photoeffect is independent of the frequency of the switched radiation, the laser, which is used in the switch of the 70-GHz radiation, will also fit the switch of the 260-GHz radiation. However, successful batch production of the switch is expected to make sense in the case of using much smaller IR lasers with a wavelength of 1.06 μm (or their second harmonic with a wavelength of 0.53 μm), the pulse duration ranging from 10 to 100 ns, and the pulse energy ranging from 10 nJ to 1 μJ.

In the subterahertz range, the switch can be a successful alternative to promising metamaterials [14, 15].

This work was supported by the Russian Scientific Foundation (project No. 14–29–00192).

REFERENCES

1. L. I. Kats and A. A. Safonov, *Interaction of Electromagnetic Oscillations of Microwave Frequencies with the Plasma of Charge Carriers in the Semconductor* [in Russian], Saratov Univ. Press., Saratov (1979).
2. O. Madelung, *Semiconductors: Data Handbook*, Springer, New York (2004).
3. G. G. Denisov, A. V. Chirkov, V. I. Belousov, et al., *J. Infrared, Millim. Terahertz Waves*, **32**, No. 3, 343 (2011).
4. M. L. Kulygin, G. G. Denisov, Yu. V. Rodin, et al., "Laser-pulse-controlled nanosecond semiconductor modulator of the 66–72 GHz microwave radiation," Preprint No. 796 [in Russian], Inst. Appl. Phys., Nizhny Novgorod (2010).
5. M. L. Kulygin, G. G. Denisov, and Yu. V. Rodin, *Tech. Phys. Lett.*, **37**, No. 4, 368 (2011).
6. A. Taflove, *Computational Electrodynamics: the Finite-Difference Time-Domain Method*, Artech House, Boston (1995).
7. S. D. Gedney, *IEEE Trans. Antennas Propagat.*, **44**, No. 12, 1630 (1996).
8. M. L. Kulygin, "Numerical modeling of 3D multimode electrodynamic eystems of electronic microwave devices," Ph. D. Theses [in Russian], Nizhny Novgorod (2006).
9. M. L. Kulygin, G. G. Denisov, and Vl. V. Kocharovsky, "Modeling of dynamical effects in the semiconductor switch of high-power microwaves," Preprint No. 747 [in Russian], Inst. Appl. Phys., Nizhny Novgorod (2007).
10. M. L. Kulygin, G. G. Denisov, and Vl. V. Kocharovsky, *J. Infrared, Millim. Terahertz Waves*, **31**, No. 1, 31 (2010).
11. M. Kulygin and G. Denisov, *J. Infrared, Millim. Terahertz Waves*, **33**, No. 6, 638 (2012).
12. G. G. Denisov, G. I. Kalynova, and D. I. Sobolev, *Radiophys. Quantum Electron.*, **47**, No. 8, 615 (2004).
13. S. V. Kuzikov and M. E. Plotkin, *Radiophys. Quantum Electron.*, **52**, No. 3, 196 (2009).
14. H.-T. Chen, J. F. O'Hara, A. K. Azad, et al., *Laser Photon. Rev.*, **5**, No. 4, 513 (2011).
15. D. B. Schrekenhamer, K. L. Burch, N. P. Butch, et al., *Opt. Express*, **19**, No. 10, 9969 (2011).